PROCEEDINGS OF SCIENCE

Ultra-deep sub-arcsec 5 GHz JVLA observations of GOODS-N: the nature of the radio emission in the faint radio source population

Daria Guidetti[*1], **Marco Bondi**[1], **Isabella Prandoni**[1], **Robert J.Beswick**[2], **Thomas W.B. Muxlow**[2], **N. Wrigley**[2], **Ian Smail**[3] **and the eMERGE collaboration**

[1] *Observatory of Radio Astronomy - INAF, Bologna;* [2] *Jodrell Bank Centre for Astrophysics, Alan Turing Building, University of Manchester, Oxford Road, Manchester, M13 9PL, UK;* [3] *Institute for Computational Cosmology, Durham University, Durham, DH1 3LE, UK*
E-mail: guidetti@ira.inaf.it

Here we present the first catalogue of radio sources in GOODS-N based on ultra deep JVLA observations at 5.5 GHz with sub-arcsec resolution. Near-IR identifications were obtained using available deep K_s-band observations, while IR colors were used to tentatively separate AGN from star-forming galaxies and passive elliptical galaxies. For the three classes of objects we present a preliminary analysis by their radio spectral properties. This work is part of the eMERGE legacy project, whose goal is to obtain a ultra-deep (sub-μJy rms), sub-arcsec (50-200 mas) imaging of the GOODS-N region at 1.4 and 5 GHz using combined JVLA and *e*MERLIN observations. Such dataset will be exploited to provide a resolved view of the GOODS-N radio source population in the high-redshift Universe where AGN cores can be spectro-morphologically separated from star forming galaxies.

EXTRA-RADSUR2015 (*)
20–23 October 2015
Bologna, Italy

(*) This conference has been organized with the support of the Ministry of Foreign Affairs and International Cooperation, Directorate General for the Country Promotion (Bilateral Grant Agreement ZA14GR02 - Mapping the Universe on the Pathway to SKA)

[*]Speaker.

© Copyright owned by the author(s) under the terms of the Creative Commons Attribution-NonCommercial-NoDerivatives 4.0 International License (CC BY-NC-ND 4.0).

PoS(EXTRA-RADSUR2015)023

1. Introduction

A complete census of both star formation and nuclear activity over cosmic time is crucial to understand the assembly and evolution of galaxies and super-massive black holes, as well as the role of mergers and secular process in driving their growth. Attempts to derive the star formation and accretion histories through optical, near-IR and X-ray surveys suffer significant uncertainties because of the large and mostly unconstrained corrections for dust extinction and gas obscuration. Even the deepest X-ray surveys may fail to detect the most heavily absorbed Compton thick AGNs. Radio continuum imaging is a powerful dust and obscuration-free tool to get unbiased measures of both star formation and AGN activity up to high redshift. and the unexpected detection of large numbers of "radiative-mode" AGNs (typically radio-quiet) in such surveys (e.g. [1]) has opened the exciting perspective of studying the whole AGN population through deep radio surveys.
Assessing the faint AGN component in deep radio fields will provide an important tool to understand the role of nuclear activity in distant galaxies, the nature and accretion regime of low-power and radiative-mode AGNs, and their possible co-evolution with star-formation processes. The nature of the radio emission in radiative-mode AGN is hotly debated, although recent works are suggesting star formation related processes (e.g. [2, 3, 1]). The most direct way to identify faint AGN-driven radio emission is the detection of embedded radio cores in the host galaxies, through ultra-deep and very high resolution radio observations.
The eMERGE survey (eMERlin Galaxy Evolution survey, [4]) is an *e*MERLIN legacy project whose goal is to obtain a resolved view of the radio source population up to high z in the Great Observatories Origins Deep Surveys-North (GOODS-N, [5]), for which a plenty of deep multi-wavelength data is available. eMERGE is based on the combination of ultra-deep *e*-MERLIN and Jansky Very Large Array (JVLA) observations at 1.4 and 5.5 GHz, and, when ultimated, will provide sub-microJy sensitivity with angular resolution on scales going from 50 mas up to a few arcsec. These correspond to linear scales from sub-kpc up to tens of kpc at $z > 1$. eMERGE will be able to properly map and distinguish compact components such as nuclei and jets ($\ll 1$ kpc), associated with nuclear activity, from more diffuse emission (> 1 kpc), indicating star formation processes. In this paper, we present preliminary results from the first catalogue of radio sources in GOODS-N based on ultra deep JVLA observations at 5.5 GHz with sub-arcsec resolution, which are part of the eMERGE legacy project. Near-IR identifications were obtained from available ultra-deep K_s-band observations and IR colors were used to tentatively separate AGNs from star-forming galaxies and passive elliptical galaxies.

2. The hybrid system J123649+620737

To give a flavor of what will be possible to do with the eMERGE survey, in this section we show the case of a ultra-luminous infrared galaxy (ULIRG) identified as possible composite system at $z \sim 2$ ([10]). Multiwavelength observations suggest the presence of both star formation and AGN activities. First of all, the optical/NIR spectra of the host galaxy display features that are consistent with a starburst at $z = 2.2$ ([6]), while do not exhibit the typical lines associated to AGN activity (for instance the C_{IV} $\lambda = 1549$ absorption line). Substantial ongoing star formation is also suggested by the CO detection of a large $10^{10} M_{\odot}$ molecular gas reservoir ([7]). Radio emission extended

PoS(EXTRA-RADSUR2015)023

over about 8 kpc, a bit larger than the size of the host galaxy, with no evidence for a compact core, was found by 1.4 GHz MERLIN observations ([8]) at 0.3 arcsec resolution. On the other hand, the presence of an AGN is suggested by the strong X-ray luminosity (1.3×10^{45} erg/s in the Chandra hard band [2-10 keV]), by the very bright and compact optical nucleus and finally by the fact that the radio emission exceeds that expected by pure star formation processes, when applying the well known radio-FIR correlation holding for star forming galaxies ([9]). By using the 1.4 GHz MERLIN data to remove a possible AGN contribution to the overall radio flux density, a SFR of $\sim 4000 M_{\odot} yr^{-1}$ was derived ([11]).

We observed this source at 5 GHz and with 0.2 arcsec FWHM during the early commissioning operations of *e*MERLIN in August 2011 ([12]) Fig. 1 shows the contours of the radio emission seen at 1.4 GHz by MERLIN (green) and at 5 GHz by eMERLIN (white) overlaid onto the Hubble Space Telescope (HST) *i* band image.

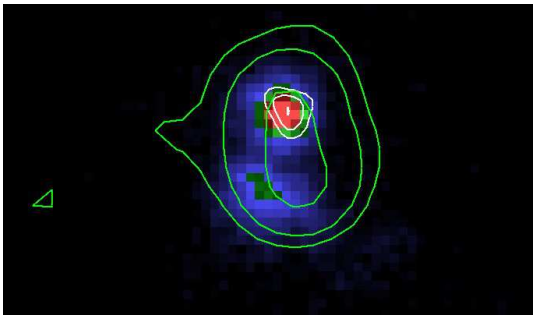


Figure 1: Radio continuum contours from 0.3 arcsec MERLIN data at 1.4 GHz (green, [8]) and from 0.2 arcsec eMERLIN data at 5.5 GHz (white, [12]) overlaid on HST ACS i-band imaging for the ULIRG source J123649+620737

The 5 GHz eMERLIN observations allowed us to better identify the compact radio core which appears coincident with the bright optical nucleus, and henceforth disentangle the AGN-related emission from the possible star forming component. We measured a 5 GHz AGN flux density of 170 μJy and, under the conservative assumption of a flat spectral index ($\alpha = 0$, assuming $S(\nu) \propto \nu^{-\alpha}$), derived a SFR$\leq 2800 M_{\odot} yr^{-1}$, at least 30%, lower than the previous estimate [10].

3. JVLA observations & imaging

We obtained new Jansky Very Large Array (JVLA) observations of GOODS-N in the 4.5–6.5 GHz frequency range (total observing time of 14 hrs in A- and 2.5 hrs in B-arrays). The observations consist of a mosaic of 7 pointings (Fig. 2 left), separated by $\sim$2 arcmin, whose geometry is optimized in view of the combination with future 5.5 GHz e-MERLIN observations, including the Lovell telescope, characterized by a smaller primary beam than the JVLA antennas.

The data were calibrated and edited using the AIPS software package, developed by the National Radio Astronomy Observatory[1], following standard procedures. The A-array and B-array datasets were edited and calibrated separately. The point-like source 3C 286 was used for the the bandpass and amplitude flux density calibration, while sources J1407+28297 and J124129+6020 for delay and phase calibration, respectively. Finally, the edited and calibrated (*u, v*) A- and B-array data were combined together and the field was imaged at an angular resolution of 0.5 arcsec.

[1]The National Radio Astronomy Observatory is a facility of the National Science Foundation operated under cooperative agreement by Associated Universities, Inc.

PoS(EXTRA-RADSUR2015)023

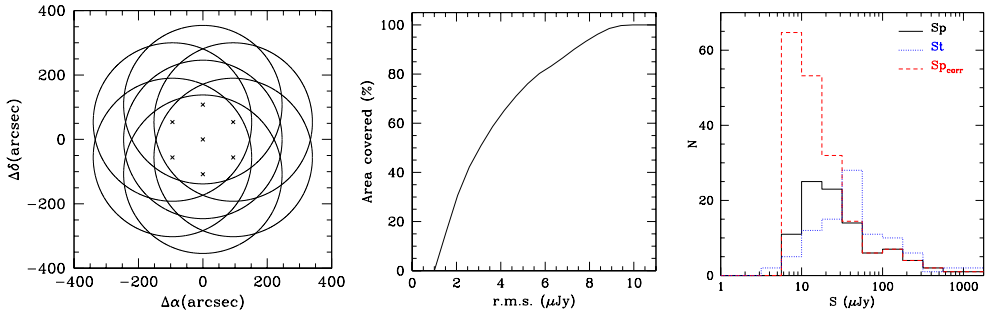


Figure 2: Left: mosaic pattern of the 7 pointing centers (crosses) at 5.5 GHz. The full circles show the primary beam of the JVLA (∼10 arcmin) at this frequency. The plot clearly illustrates that the region observed is oversampled. The J2000 coordinate of the central pointing are $\alpha = 12^{\rm h}36^{\rm m}49^{\rm s}.4$, $\delta = +62^{\circ}12'58''$. Center: visibility function of the 5.5 GHz mosaic (area vs rms sensitivity) calculated over the region used to derive the source catalog (see text). Right: observed peak (continuous black line) and total flux densities (dotted blue line) distribution of the 5.5 GHz sources. The dashed red line indicates the peak flux density histogram after correcting for the visibility function.

We imaged the whole bandwidth simultaneously using the multi-scale multi-frequency (MSMF) synthesis clean algorithm available in the CASA package that takes into account the frequency-dependent variations over the observing band (e.g. [13], [14]). The resulting image was then corrected for the primary beam and the final mosaic obtained by a weighted combination of the seven pointings in AIPS. Finally, a noise image of the mosaic was generated as well. Fig. 2 (center) shows the visibility function of the 5.5 GHz mosaic: the rms noise is $\leq 3\mu$Jy over about 50% of the mapped area and remains $\leq 10\mu$Jy across the whole field.

4. Source catalogue

In a circular region of radius 7 arcmin around the mosaic center, we extracted a catalogue of 94 sources with local signal-to-noise ratio$\geq$ 5 (SNR, defined as the ratio between the source peak flux density and the local noise), following the standard approach of other radio surveys (e.g. [15]). Peak and total flux densities, source position and size were measured through a Gaussian fit and a simple cubic interpolation for high and low SNR components, respectively. The peak (Sp) and total flux density (St) distributions for the catalogued objects are shown in Fig. 2 (right). Half of the sources have S_p in the range $10-30$ μJy/beam, and only 16% have $Sp > 100$ μJy/beam. Finally, 59 (35) sources are considered extended (point-like) on the basis of the peak-to-extended flux density ratio distribution. The median deconvolved angular size of the sources is 0.4 arcsec, corresponding to ~ 3 kpc at the median redshift of the catalogue (see Sect. 5).

5. NIR identifications & redshift

We cross-matched our catalogue with two available ultra-deep *Ks*-band catalogues ([16], 5σ $K_{s,AB} \leq 24.45$; [17], 5σ $K_{s,AB} \leq 25$). The first one entirely covers our 5.5 GHz mosaiced area, while the second one is slightly deeper but only partially covers our field of view. 82/94 sources of our 5.5 GHz catalogue have a secure *Ks*-band association. No significant systematic offset between the

PoS(EXTRA-RADSUR2015)023

radio and near-IR positions was found.
The sources with no reliable NIR counterpart (12/94) could be either distant/intrinsically faint NIR sources, NIR obscured systems or perhaps false radio detections. Indeed, most of them have low SNR (<5.5) at 5.5 GHz. In the literature we found redshift information for 75/94 objects (55 with spectroscopic measures: [18, 19, 20] and reference therein; 20 with photometric estimates: [17, 21]). Hereafter we use spectroscopic redshifts where available, and photometric redshifts otherwise. The redshift distribution appears bimodal: there is a first peak around $z \simeq 0.6$ and a less prominent one around $z \simeq 2$. One object is a local galaxy at $z < 0.1$. The median redshift of the 5.5 GHz sources is $z = 1.14$ ($z = 0.86$ considering only spectroscopic redshifts).

6. InfraRed color diagnostics

A large number of methods are currently used to classify radio sources as AGN, star forming or quiescent galaxies. Some of them rely on IR color-color classification criteria which have proved to be powerful to identify AGN and bright, low-redshift star-forming galaxies (e.g. [22, 23],[24]). However, for samples characterized by sources spanning a wide range of redshift (as for our catalogue), it is essential to take into account the color evolution with redshift to avoid mis-classifications (e.g. [25].
We applied 5 different IR color-color criteria [24, 25, 26, 27] to our 5.5 GHz sources. These are based on different combination of IRAC, FIR and Ks-band photometry and some of them account for color evolution. IRAC data in all the four bands ([16]) are available for 74 radio sources with NIR identification. Sixty-five sources have also an entry in the GOODS-N-*Herschel* catalogue ([28]).

Here we show one color-color plot (Fig. 3), which summarizes the source classification from all the IR criteria, used in this work. In such diagram, we overplot the original selection wedge by [23] together with the IRAC color cuts used by [26] as a simple approximation for the revised power-law AGN wedge proposed by [25].
As far as our sample is concerned, the [25, 26] selection criteria are equivalent. Indeed, all the 13 radio sources that fall within these two color cuts have IRAC flux densities monotonically increasing with wavelength.

We found that 36 objects are classified as AGN candidates by at least one of the five IR color-color criteria, 24 of which are selected as such by at least two different IR criteria. We classify a group of 14 radio sources as passive galaxies having mid-IR colors consistent with quiescent galaxies at $z \sim 1 - 1.5$ (see [25]). Finally, 24 sources do not fit in the AGN selection region of any of the used IR color-color plots. This does not mean that all these sources are star-forming galaxies, as most of the IR criteria used here are conservative at expense of completeness. These objects could be either pure star forming galaxies, or hybrids systems not AGN-dominated, or high-z quiescent galaxies. In the following, we will refer to them as SF/comp systems.
The optical morphology of the host galaxies seem to confirm our IR classifications: optically bright and compact cores are seen in the IR AGN population; the counterparts of the passive galaxies have early-types morphology. Interestingly, many of SF/comp hosts show disturbed morphologies or ongoing mergers. Examples are shown in Fig 4.

PoS(EXTRA-RADSUR2015)023

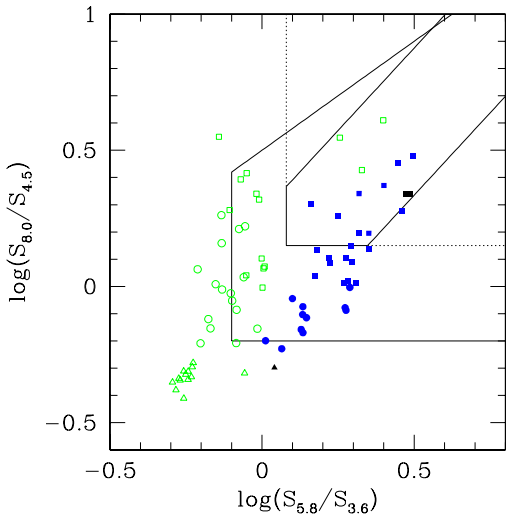


Figure 3: IRAC colors of GOODS-N sources detected at 5.5 GHz. The larger wedge shows the original AGN selection region [23]; the smaller one is the revised wedge effective in selecting power-law AGN [25] and the dotted lines show the IRAC color cuts proposed by [26]. Sources at $z < 1.5$ are shown with empty green symbols and sources with $z > 1.5$ as filled blue symbols. The black ones have no measured redshift. Squares symbols are used to indicate sources which are classified as candidate AGN by at least one of the other IR criteria. Triangles identify candidate passive elliptical galaxies.

7. Radio spectral properties

So far, the deepest published GOODS-N catalogue at GHz frequencies is the 1.4 GHz catalogue by [15], which contains 1230 radio sources with completeness limit of $\sim$20 μJy (5σ) at the field center. The angular resolution of these 1.4 GHz observations is 1.7 arcsec and the rms noise goes from $\sim$3.9 μJy at the phase center up to $\sim$8 μJy 15 arcmin outwards. Our 5.5 GHz mosaic area is entirely covered by such observations and 76/94 of our sources have a counterpart in the 1.4 GHz catalogue by [15].

We performed a spectral index analysis between 1.4 and 5.5 GHz for a sub-sample of radio sources (61/94) whose 1.4 GHz deconvolved angular size is $\leq$ 1 arcsec ($\leq$8 kpc at the median z of our sample). This guarantees similar surface brightness sensitivities at the two radio frequencies. At the rest-frame frequencies (ν_{rf}) probed by our data (spanning the range $1 \geq \nu_{rf} \leq 30$ GHz), radio emission with flat/inverted spectral index ($\alpha \leq 0.5$) is most likely powered by an AGN. While star-forming galaxies and high-redshift sub-millimeter galaxies dominated by non-thermal, optically thin synchrotron emission usually show steeper spectra (i.e. $\alpha \sim 0.8$, [11], [29]). Fig. 5 shows the spectral index distribution of the three groups of IR-classified sources. IR AGN candidates are characterized on average by steep spectra (median $\alpha \sim 0.72$, rest-frame $\nu \leq 30$ GHz) indicating optically thin syncrothron emission. None of them show inverted spectra. These results are consistent with what found by [30] and might suggest a radio emission dominated by star formation. Alternatively, a steepening of intrinsically flat spectra might be a k-correction effect, although we do not see evidence for a redshift evolution of the spectral index in our sample. Passive galaxies have on average much flatter spectra (median $\alpha \sim 0.04$, rest-frame $\nu \leq 10$ GHz), with a peak at $\alpha \sim 0$, suggesting a relative large fraction of self-absorbed radio AGN cores, as observed in many local FRI radio galaxies (e.g. [31]). These quiescent galaxies might be the high-z, compact counterparts of classical extended FRI radio galaxies. We notice that similar results were found by [32] for a brighter sub-mJy sample ($S_{5\,GHz} \geq 0.4$ mJy).

The spectral distribution of the SF/comp systems is steep and does not show any particular peak. This is symptomatic of a mixture of radio emission processes, and is somewhat expected consider-

PoS(EXTRA-RADSUR2015)023

ing the uncertain IR classification. One point which has to be stated very clear is that our spectral index measurements refer to similar intrinsic spatial scales for all the three classes of IR objects, given the similar median redshift.

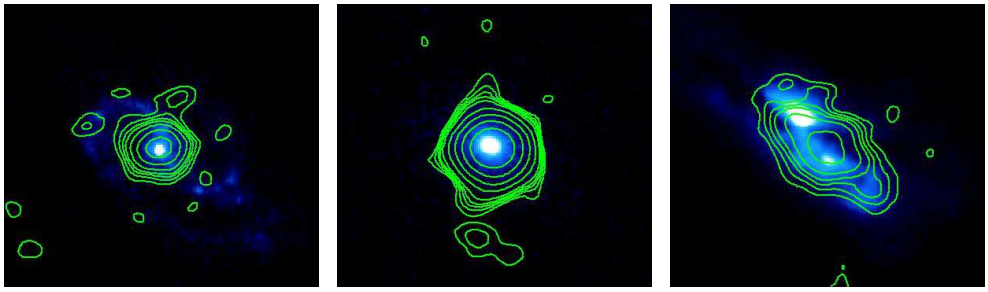


Figure 4: 5.5 GHz contours overlaid on the HST B-band images for an IR-AGN candidate (left), a passive galaxy (center) and a SF/Comp system (right).

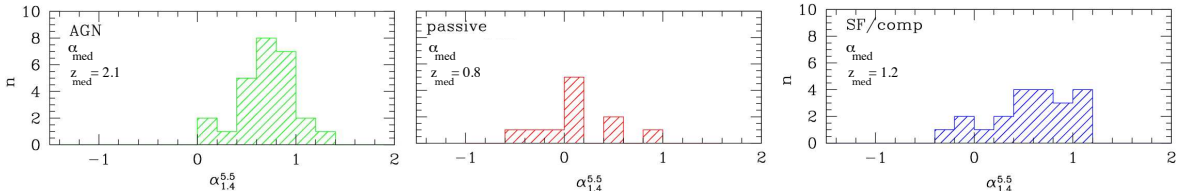


Figure 5: Spectral index distribution of the three groups of IR classified sources. The median $\alpha_{1.4}^{5.5}$ and redshift z are given in each panel.

8. Summary & Future perspectives

We have presented an ultra-deep sub-arcsec-resolution radio mosaic of GOODS-N at 5.5 GHz and a catalogue of 94 radio sources extracted in the central 7 arcmin diameter field. This work is part of the eMERGE legacy project. Our mosaic represents the most sensitive survey with sub-arcsec resolution undertaken so far at 5 GHz. By applying IR color-color criteria, 36 sources are presumably radiative-mode AGNs and 14 sources are associated to passive early-type galaxies, presumably radio mode AGNs. On the basis of a first spectral index analysis we suggest star formation as the dominant process in our radiative-mode AGNs. However, as our spectral indices refer to kpc scale radio emission, we cannot rule out the presence of flat-spectrum cores at the center of their host galaxies. Nevertheless, given the steep radio spectra, these cannot be dominant. The higher angular resolution provided by future *e*-MERLIN observations ($\sim$ 50 mas) will be crucial to pinpoint AGN cores in the faint GOODS-N source population and provide a truly unbiased view of AGN and SF processes at high redshift.

References

[1] Bonzini, M., Padovani, P., Mainieri, V., et al. 2013, MNRAS, 436, 3759

[2] Padovani, P., Miller, N., Kellermann, K. I., et al. 2011, ApJ, 740, 20

PoS(EXTRA-RADSUR2015)023

[3] Condon, J. J., Cotton, W. D., Fomalont, E. B., et al. 2012, ApJ,758, 23

[4] Muxlow T. W. B., Smail I. R., McHardy I., 2008, E-Merge Consortium, Proc. 9th European VLBI Network Symp., p. 22, available at: http://pos.sissa.it/cgi-bin/reader/conf.cgi?confid=72

[5] Giavalisco, M., Ferguson, H. C., Koekemoer, A. M., et al. 2004, ApJ,600, 93

[6] Chapman S. C., Smail I., Blain A. W., Ivison R. J., 2004a, ApJ, 614, 671

[7] Chapman, S. C., Neri, R., Bertoldi, F., Smail, I., et al. 2008,ApJ, 689, 889

[8] Muxlow T. W. B, et al., 2005, MNRAS, 358, 1159

[9] Del Moro, A., Alexander, D. M., Mullaney, J. R., et al., 2013, A&A, 549, 59

[10] Casey C. M. et al., 2009, MNRAS, 399, 121

[11] Condon, J. J., 1992, AR&A, 30, 575

[12] Guidetti, D., Bondi, M., Prandoni, I., et al., MNRAS, 432, 2798

[13] Rau, U. & Cornwell, T. J., 2011, A&A, 532, 71

[14] Rau, U., Bhatnagar, S., Owen, F.N., 2014arXiv1403.5242R

[15] Morrison G. E., Owen F. N., Dickinson M., Ivison R. J., Ibar E., 2010, ApJS, 188, 178

[16] Wang, W.H., Cowie, L.L., Barger, A. J., 2010, ApJS, 187, 251

[17] Kajisawa, M., Ichikawa, T., Tanaka, I., 2011,PASJ, 63, 379

[18] Barger, A. J., Cowie, L. L., Wang, W.-H., 2008, ApJ, 689, 687

[19] Wirth, G.D., Willmer, C. N. A., Amico,P., 2004, AJ, 127, 3121

[20] Cowie, L. L., Barger, A. J., Bautz, M. W., et al., 2001, Apj, 551, 9

[21] Skelton, R.E., Whitaker, K. E., Momcheva, I. G., et al. 2014, ApJS, 214, 24

[22] Lacy, M., Storrie-Lombardi, L. J., Sajina, A., et al., 2004, ApJS, 154, 166

[23] Lacy, M., Petric, A. O., Sajina, A., Canalizo, G., et al. AJ, 133, 186

[24] Stern, D., Eisenhardt, P., Gorjian, V., et al., 2005, ApJ, 631, 163

[25] Donley, J. L., Koekemoer, A. M., Brusa, M., et al. 2012, ApJ, 748, 142

[26] Kirkpatrick, A., Pope, A., Alexander, D. M., et al., 2012, ApJ, 759, 139

[27] Messias, H., Afonso, J., Salvato, M. et al., 2012, ApJ, 754, 120

[28] Elbaz, D., Dickinson, M., Hwang, H. S., et al., 2011, A&A, 533, 119

[29] Ibar, Ed., Ivison, R. J., Best, P. N., Coppin, K., 2010, MNRAS, 401, 53

[30] Magnelli, B., Lutz, D., Saintonge, A., et al. 2014, A&A, 561, 86

[31] Laing, R. A., Guidetti, D., Bridle, A. H., et al. 2011, MNRAS, 417, 2789

[32] Mignano, A., Prandoni, I., Gregorini, L. et al. 2008, A&A, 477, 459

PoS(EXTRA-RADSUR2015)023